Bulk waves in phononic crystals

Examples of phononic crystals

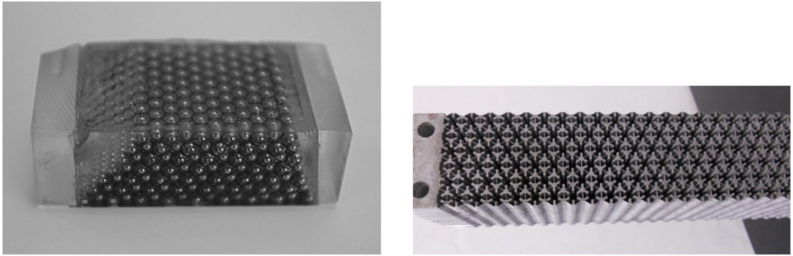

(a) (b)

Figure: **Examples of phononic crystals.** (a) 3D phononic crystal of steel spheres in an epoxy matrix arranged according to a FCC lattice [8]. (b) 2D phononic crystal of holes in aluminum [9].

Elastodynamic equations

- Dynamic equation

$$T_{ij,j} + f_i = \rho \frac{\partial^2 u_i}{\partial t^2}$$

- $\mathbf{u}$ is the displacement vector, T_{ij} is the stress tensor
- f_i are body forces (often, sources)
- Constitutive equation of elasticity (Hooke's law)

$$T_{ij} = c_{ijkl} S_{kl}$$

  with c_{ijkl} the elastic tensor and $S_{ij} = \frac{1}{2}\left(u_{i,j} + u_{j,i}\right)$ the strain tensor.
- Contracted notation: $I = (ij)$ for any pair of symmetric indices. $I = 1 \cdots 6$. $T_I = c_{IJ} S_J$.
- In phononic crystals, the material tensors are discontinuous functions of position.

Independent elements of the elastic tensor c_{IJ}

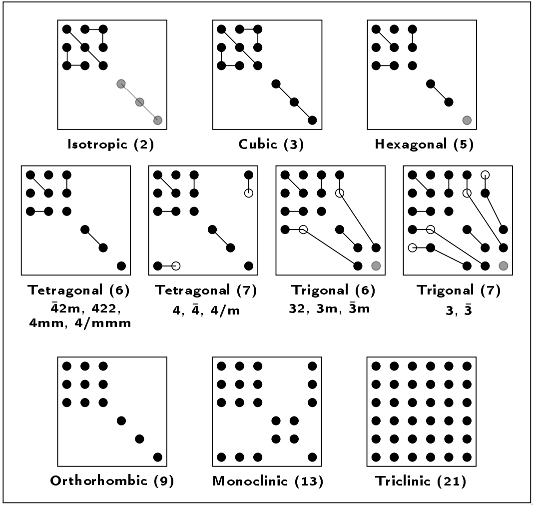

Elastic constants for selected solids

Material	Point group	Elastic constants (10^{10} N/m^2)						ρ (10^3 kg/m^3)
Iso.		c_{11}	c_{44}					
SiO_2	-	7.85	3.12					2.203
Cubic		c_{11}	c_{12}	c_{44}				
AsGa	$\bar{4}3m$	11.88	5.38	2.83				5.307
Si	$m3m$	16.56	6.39	7.95				2.329
Hexa.		c_{11}	c_{12}	c_{13}	c_{33}	c_{44}		
PZT-4	-	13.9	7.8	7.4	11.5	2.6		7.5
ZnO	$6mm$	21.0	12.1	10.5	21.1	4.2		5.676
Tetra.		c_{11}	c_{12}	c_{13}	c_{33}	c_{44}	c_{66}	
TiO_2	4/mmm	26.6	17.3	13.6	47.0	12.4	18.9	4.28
Trigonal		c_{11}	c_{12}	c_{13}	c_{33}	c_{44}	c_{14}	
Al_2O_3	$\bar{3}m$	49.7	16.3	11.1	49.8	14.7	-2.3	3.986
$LiNbO_3$	$3m$	20.3	5.3	7.5	24.5	6.0	0.9	4.7
quartz-α	32	8.7	0.7	1.2	10.7	5.8	-1.8	2.648

Attenuation

When loss must be taken into account, a practical model is viscoelasticity: the elastic tensor becomes complex-valued and dispersive

$$\boxed{c_{IJ} \longrightarrow c_{IJ} + \imath\omega\eta_{IJ}}$$

Table: **Phonon viscosity tensor η_{IJ} for some materials and crystals.**

Material	Point group	Phonon viscosity constants $(10^{-3}\ \mathrm{N/m^2.s})$					
Iso.		η_{11}	η_{44}				
SiO_2 [10]	-	5.9	≈ 0.6				
Cubic		η_{11}	η_{12}	η_{44}			
AsGa [11]	$\bar{4}3m$	7.49	6.57	0.72			
Si [11]	$m3m$	5.9	5.16	0.62			
Trigonal		η_{11}	η_{12}	η_{13}	η_{33}	η_{44}	η_{14}
$LiNbO_3$ [12]	$3m$	0.6547	0.2275	0.2499	0.3377	0.1765	-0.0687
quartz-α [10]	32	1.37	0.73	0.71	0.96	0.36	0.01

Weak form of the elastodynamic equation, boundary conditions

- Consider test functions $\mathbf{v}$ that are defined on the same finite element space as the displacement vector $\mathbf{u}$. Projection on the test functions results in

$$-\int_{\Omega} d\mathbf{r}\ \mathbf{v}^* \cdot (\nabla \cdot T) + \int_{\Omega} d\mathbf{r}\ \mathbf{v}^* \cdot \rho \frac{\partial^2 \mathbf{u}}{\partial t^2} = \int_{\Omega} d\mathbf{r}\ \mathbf{v}^* \cdot \mathbf{f}$$

- Apply the divergence theorem and insert Hooke's law to get

$$\int_{\Omega} d\mathbf{r}\ S(\mathbf{v})_I^* c_{IJ} S(\mathbf{u})_J - \int_{\sigma} d\mathbf{s}\ \mathbf{v}^* \cdot T_n + \int_{\Omega} d\mathbf{r}\ \mathbf{v}^* \cdot \rho \frac{\partial^2 \mathbf{u}}{\partial t^2} = \int_{\Omega} d\mathbf{r}\ \mathbf{v}^* \cdot \mathbf{f}$$

  $T_n = T_{ij} n_j$ is the normal traction.
- External boundary conditions – free: $T_n = 0$; Dirichlet: $u_i = u_{0i}$
- Continuity between elements of displacements and normal tractions.

FEM for a unit-cell: the band structure of phononic crystals

Apply periodic boundary conditions and consider Bloch waves as $u_i(t,\boldsymbol{x}) = \tilde{u}_i(\boldsymbol{x})\exp(\imath(\omega t - \boldsymbol{k}\cdot\boldsymbol{x}))$

$$\int_\Omega d\mathbf{r}\ S(\mathbf{v})_I^* c_{IJ} S(\mathbf{u})_J = \omega^2 \int_\Omega d\mathbf{r}\ \mathbf{v}^* \cdot \rho\mathbf{u}$$

where the strains should be understood as

$$S_1(\mathbf{u}) = \frac{\partial \tilde{u}_1}{\partial x_1} - \imath k_1 \tilde{u}_1,$$

$$S_2(\mathbf{u}) = \frac{\partial \tilde{u}_2}{\partial x_2} - \imath k_2 \tilde{u}_2,$$

$$S_3(\mathbf{u}) = \frac{\partial \tilde{u}_3}{\partial x_3} - \imath k_3 \tilde{u}_3,$$

$$S_4(\mathbf{u}) = \frac{\partial \tilde{u}_3}{\partial x_2} + \frac{\partial \tilde{u}_2}{\partial x_3} - \imath(k_3 \tilde{u}_2 + k_2 \tilde{u}_3),$$

$$S_5(\mathbf{u}) = \frac{\partial \tilde{u}_3}{\partial x_1} + \frac{\partial \tilde{u}_1}{\partial x_3} - \imath(k_3 \tilde{u}_1 + k_1 \tilde{u}_3),$$

$$S_6(\mathbf{u}) = \frac{\partial \tilde{u}_2}{\partial x_1} + \frac{\partial \tilde{u}_1}{\partial x_2} - \imath(k_2 \tilde{u}_1 + k_1 \tilde{u}_2).$$

2D HEX phononic crystal of steel rods in epoxy I

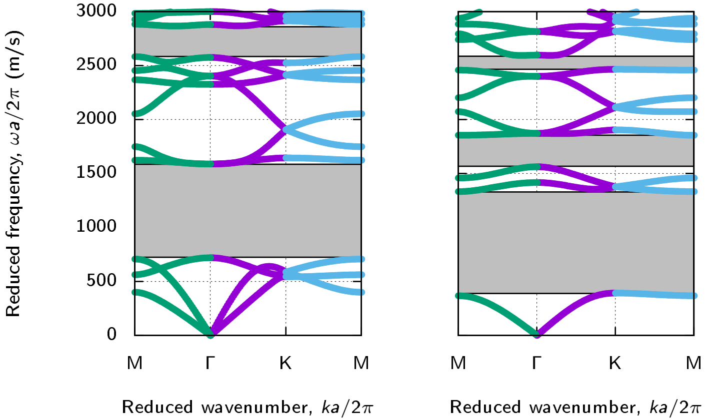

Figure: The filling fraction is $F = 0.4$ or $d/a = 0.6641$ [13].

2D HEX phononic crystal of steel rods in epoxy II

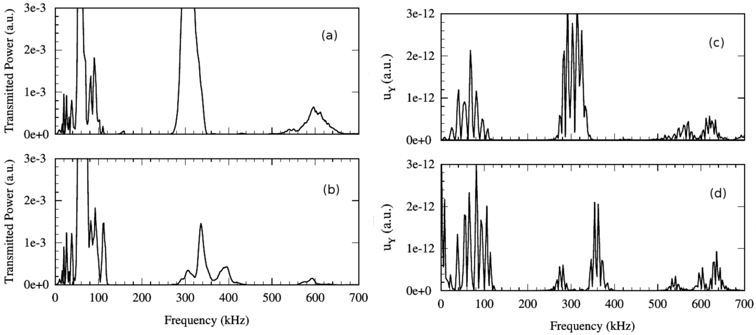

Figure: **Experimental transmission.** The filling fraction is $F = 0.4$ or $d/a = 0.6641$. The measured transmission for longitudinal waves is shown for (a) the ΓK and (b) the ΓM directions (c-d) computed transmission [13]

2D HEX-lattice phononic crystal of cylindrical holes in steel

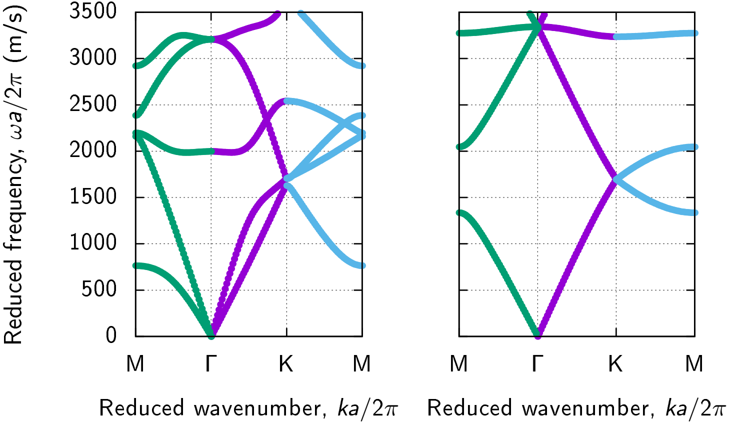

Figure: The filling fraction is $F = 0.4$ or $d/a = 0.6641$.

2D SQ-lattice phononic crystal of cylindrical holes in steel

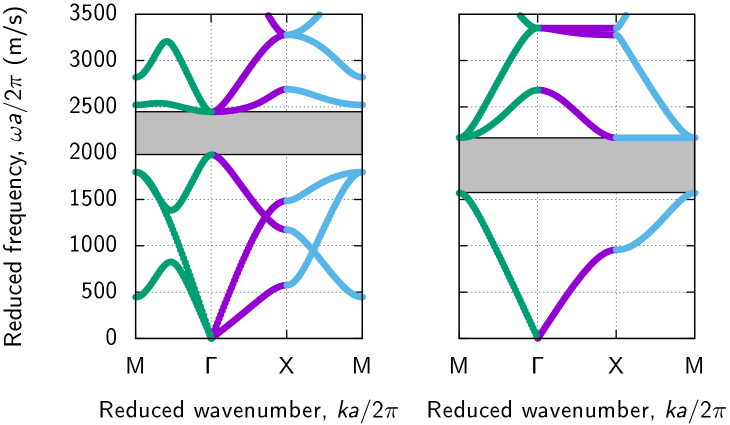

Figure: The filling fraction is $F = 0.54$ or $d/a = 0.83$.

2D HC-lattice phononic crystal of cylindrical holes in steel

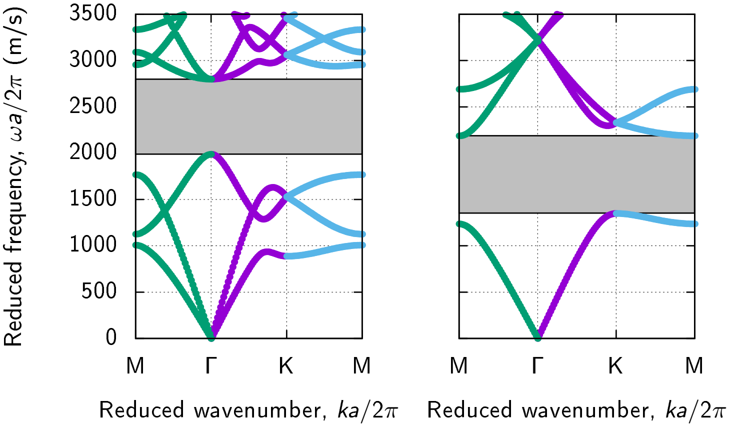

Figure: The filling fraction is $F = 0.39$ or $d/a = 0.462$.

2D SQ-lattice phononic crystal of cylindrical holes in silicon

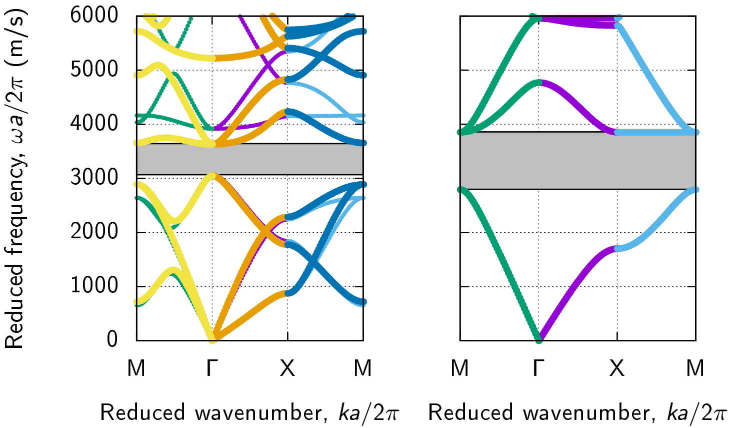

Figure: The filling fraction is $F = 0.54$ or $d/a = 0.83$. small dots: natural crystallographic orientation; large dots: 45°-rotation or [110] direction.

2D SQ-lattice phononic crystal of cylindrical holes in TiO_2

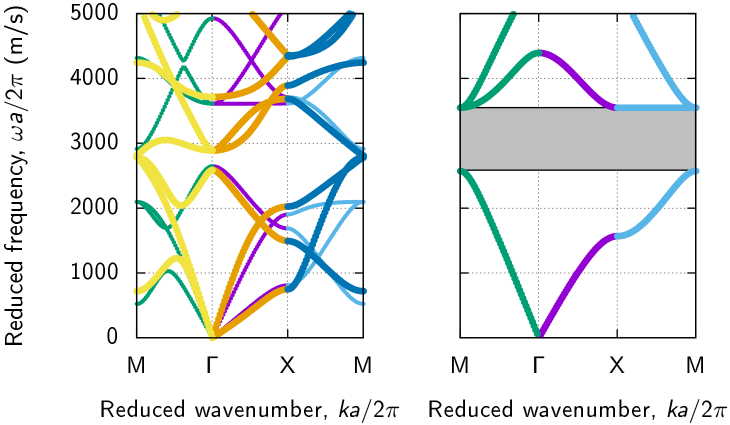

Figure: The filling fraction is $F = 0.54$ or $d/a = 0.83$. small dots: natural crystallographic orientation; large dots: 45°-rotation or [110] direction.

3D FCC-lattice phononic crystal of steel spheres in polymer

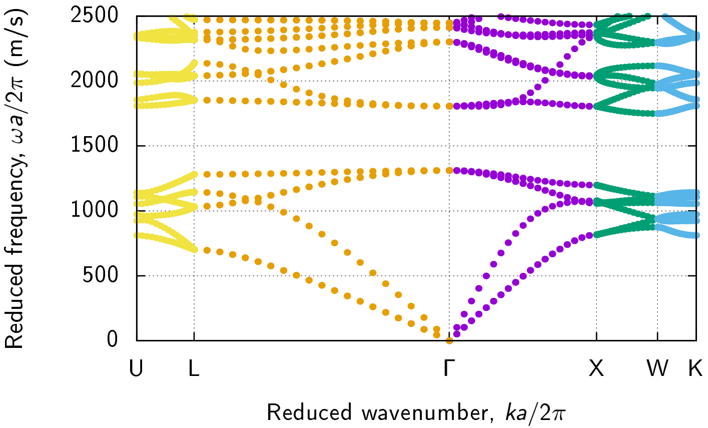

Figure: The filling fraction is $F = 0.184$ $(d/a = 0.445)$ [14].

3D FCC-lattice phononic crystal of steel spheres in epoxy

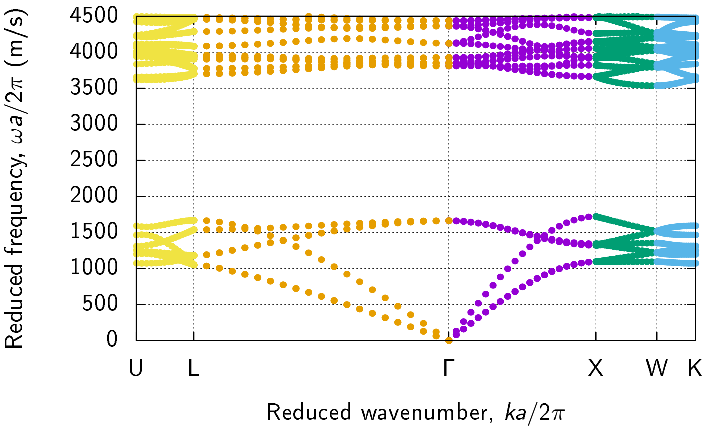

Figure: The filling fraction is $F = 0.74$ $(d/a = 0.707)$ [8].

Steel spheres in epoxy, 3D close-packed FCC

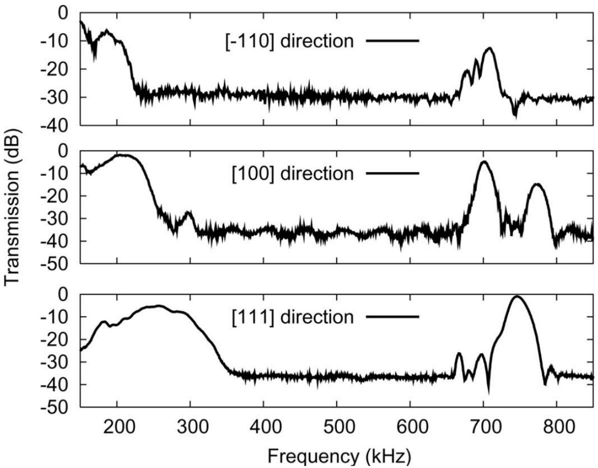

Figure: Experimental transmission power spectra along (a) the $[\bar{1}10]$, (b) the [100], and (c) the [111] directions of a 4-period PC [8].

Piezoelastic equations

Mechanical quantities are coupled with (quasi-static) electrical quantities. The most efficient formulation is the extended piezoelastic model:

$$T^e_{ij,j} = \rho^e_{ik} \frac{\partial^2 u^e_k}{\partial t^2},$$
$$T^e_{ij} = c^e_{ijkl} u^e_{k,l}.$$

with

$$\bar{c}_{ijkl} = \begin{cases} c_{ijkl} & i,l = 1,2,3 \\ e_{kij} & l = 4, i = 1,2,3 \\ e_{jkl} & i = 4, l = 1,2,3 \\ -\epsilon_{jk} & i,l = 4 \end{cases} \qquad \rho_{il} = \rho \begin{pmatrix} 1 & 0 & 0 & 0 \\ 0 & 1 & 0 & 0 \\ 0 & 0 & 1 & 0 \\ 0 & 0 & 0 & 0 \end{pmatrix}$$

and the generalized displacements, $\bar{u}_i$, and stresses, $\bar{T}_{ij}$, defined as

$$\begin{aligned} \bar{u}_i &= u_i, i = 1,2,3, \\ \bar{u}_4 &= \Phi, \\ \bar{T}_{ij} &= T_{ij}, i = 1,2,3, \\ \bar{T}_{4j} &= D_j, \end{aligned}$$

Tensors of the piezoelectric constitutive relation

$$
\begin{array}{cccccc|ccc}
c_{11} & c_{12} & \cdot & \cdot & \cdot & c_{16} & e_{11} & e_{21} & e_{31} \\
\cdot & c_{22} & \cdot & \cdot & \cdot & \cdot & e_{12} & \cdot & \cdot \\
\cdot & \cdot & \cdot & \cdot & \cdot & \cdot & \cdot & \cdot & \cdot \\
\cdot & \cdot & \cdot & \cdot & \cdot & \cdot & \cdot & \cdot & \cdot \\
\cdot & \cdot & \cdot & \cdot & \cdot & \cdot & \cdot & \cdot & \cdot \\
\cdot & \cdot & \cdot & \cdot & \cdot & c_{66} & e_{16} & \cdot & e_{36} \\
\hline
e_{11} & e_{12} & \cdot & \cdot & \cdot & e_{16} & \varepsilon_{11} & \varepsilon_{12} & \varepsilon_{13} \\
e_{21} & \cdot & \cdot & \cdot & \cdot & \cdot & \cdot & \varepsilon_{22} & \varepsilon_{23} \\
e_{31} & \cdot & \cdot & \cdot & \cdot & e_{36} & \cdot & \cdot & \varepsilon_{33}
\end{array}
$$

Material	Elastic constants $(\mathrm{C/m^2})$						Diel. constants $(10^{-11}\ \mathrm{F/m})$	
Cubic	e_{14}						ε_{11}	
AsGa	-0.16						9.73	
Hexa.	e_{13}	e_{31}	e_{33}				ε_{11}	ε_{33}
PZT-4	12.7	-5.2	15.1				650	560
ZnO	-0.59	-0.61	1.14				7.38	7.83
Trigonal	e_{11}	e_{14}	e_{13}	e_{22}	e_{31}	e_{33}	ε_{11}	ε_{33}
$LiNbO_3$	0	0	3.7	2.5	0.2	1.3	38.9	25.7
quartz-α	0.717	-0.0406	0	0	0	0	3.92	4.10

FEM for piezoelasticity

Consider a mixed finite element space for $(\boldsymbol{u}, \Phi)$. The test functions are defined in the same space and are denoted $(\boldsymbol{v}, \Psi)$. The variational formulation is based on the equation

$$-\int_\Omega \mathbf{v}^* \cdot \nabla T + \int_\Omega \mathbf{v}^* \cdot \rho \frac{\partial^2 \mathbf{u}}{\partial t^2} - \int_\Omega \Psi^* \nabla \cdot \boldsymbol{D} = \int_\Omega \mathbf{v}^* \cdot \mathbf{f}.$$

After application of the divergence theorem

$$\int_\Omega S(\mathbf{v})_I^* T_I - \int_\sigma \mathbf{v}^* \cdot T_n + \int_\Omega \mathbf{v}^* \cdot \rho \frac{\partial^2 \mathbf{u}}{\partial t^2} + \int_\Omega \nabla \Psi^* \cdot \boldsymbol{D} - \int_\sigma \Psi D_n$$
$$= \int_\Omega \mathbf{v}^* \cdot \mathbf{f}.$$

Boundary conditions are both mechanical and electrical – no surface charge: D_n; fixed potential: $\Phi = V$

2D SQ-lattice phononic crystal of holes in (ZX) $LiNbO_3$

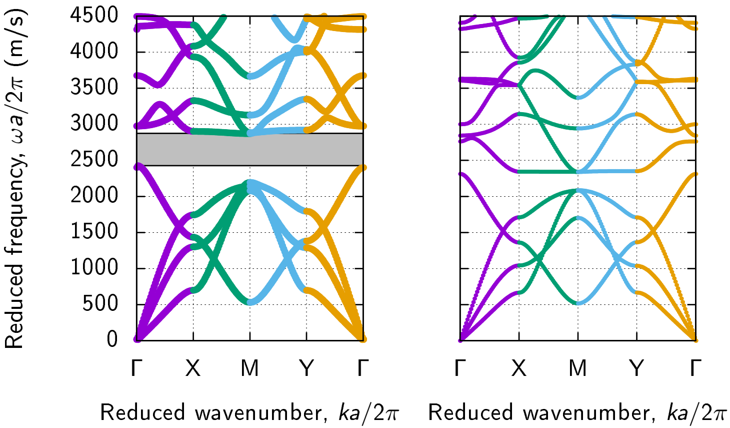

Figure: The filling fraction is $F = 0.54$ or $d/a = 0.83$. Left/right: with/without piezoelectricity taken into account.

2D SQ-lattice phononic crystal of holes in (YX) $LiNbO_3$

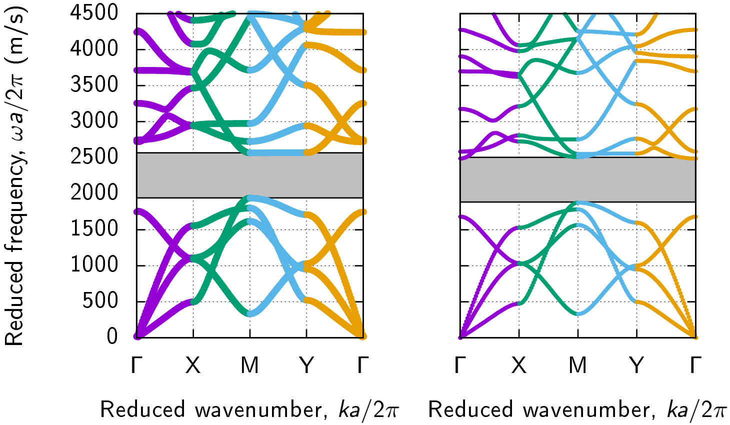

Figure: The filling fraction is $F = 0.54$ or $d/a = 0.83$. Left/right: with/without piezoelectricity taken into account.

2D SQ-lattice phononic crystal of holes in (XY) $LiNbO_3$

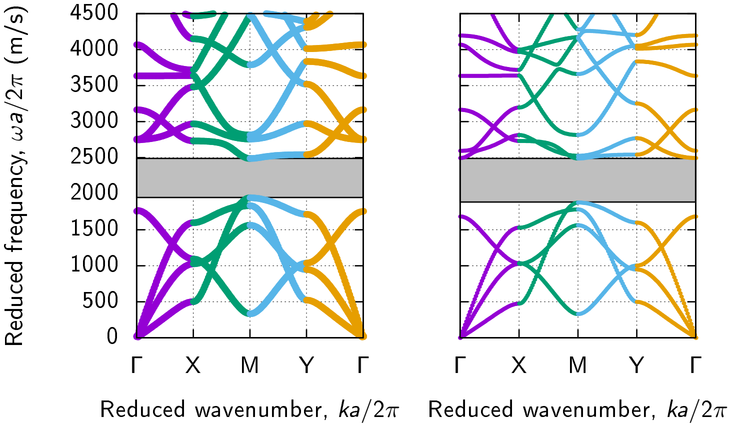

Figure: The filling fraction is $F = 0.54$ or $d/a = 0.83$. Left/right: with/without piezoelectricity taken into account.